The Eighth China-Japan-Korea Joint Symposium on Optimization of Structural and Mechanical Systems
May 25-29, 2014, Gyeongju, Korea

Paper No. 0058

Parameter Optimization of Three-Directional Tuned Mass Damper for Seismic Response Control

Toma Hasegawa[1], Makoto Ohsaki[2*] and Seita Tsuda[3]

[1]*Department of Architecture, Hiroshima University, 739-8527, Higashi-Hiroshima, Japan*
[2]*Department of Architecture, Hiroshima University, 739-8527, Higashi-Hiroshima, Japan*
** Corresponding author: ohsaki@hiroshima-u.ac.jp*
[3]*Faculty of Design, Okayama Prefectural University, 719-1197, Soja, Japan*

Abstract

An optimization approach is presented for design of a new tuned mass damper called TD-TMD for three-directional seismic response reduction of structures. The mass damper consists of a viscous damper and a mass connected by flexible springs. By utilizing the flexibility of springs, the movement of the mass in three-directions and the elongation of viscous damper are amplified, and the vibration energy of the mass is effectively absorbed by the viscous damper. The TD-TMDs are attached to a latticed roof and its seismic responses are compared with those with conventional single-directional dampers (SD-TMDs). The objective function of the parameter optimization problem is the mean norm of the response displacements at the nodes of the roof. The bounds of parameters are determined by solving a auxiliary nonlinear programming problem to maximize the minimum deformation of the damper against static loads of various directions. The parameters are discretized into integer values, and approximate optimal solutions are found using a heuristic approach called tabu search (TS) combined with pure random search (PRS) that generates efficient intial solutions.

Keywords: Tuned mass damper; Seismic response control; Pure random search; Tabu search

1. Introduction

Tuned mass damper (TMD) is effectively used for reduction of vibration due to seismic and/or wind excitations. However, a conventional TMD can reduce the responses in single direction. Therefore, several TMDs are needed for reduction of multi-directional and multi-frequency vibrations [1,2].

The authors presented a mass damper that can reduce two-directional vibration of an arch using single set of a mass and a viscous damper [3]. A TMD for three-directional control was also presented [4]; however, the mechanism of the TMD in Ref. [4] is very complicated, and the response reduction against seismic motions with various levels is not ensured, because geometrical nonlinearity is utilized.

In this study, a three-directional TMD (TD-TMD) as shown in Fig. 1 is proposed for reduction of three-directional vibration of a long-span structure subjected to multi-component ground motions.

The parameters of the TD-TMD in Fig. 1 are optimized to reduce the seismic responses, and the performances of the optimized models are verified in comparison to the structure that have single-directional TMDs (SD-TMDs) with the same total mass as the TD-TMD.

2. Description of TD-TMD and structural model

2.1 TD-TMD model

Fig.1 illustrates the proposed TD-TMD for reduction of three directional vibration. It consists of a mass, a damper, and five springs. Node A is connected to the main structure. The displacement of nodes A and C have the same values as we assume that the TD-TMD in Fig 1 is installed in a box. Nodes A and B have the same horizontal displacements.

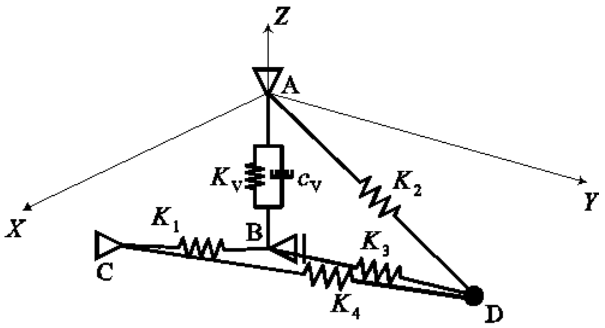

Fig. 1. Components of TD-TMD; a mass at node D, vertical viscous damper between nodes A and B, and five springs.

2.2 Seismic motion

The dynamic responses of the structure with TD-TMD are evaluated by time-history analysis using a software package called OpenSees Ver 2.4 [5]. Five artificial ground motions compatible to the acceleration response spectrum in Table 1 are used. The duration is 20 sec., and the time step for integration is 0.01 sec.

Different motions among the five motions are selected for

* Corresponding author. Tel. and Fax: +81-82-424-7794,
E-mail address: ohsaki@hiroshima-u.ac.jp

X-, Y-, and Z-directions; therefore, the total number of sets is 60. The seismic motion is scaled by 5 in X- and Y-directions, and by 2.5 in Z-direction.

Table 1. Target acceleration response spectrum (damping factor = 0.05).

Period (s)	$T \le 0.16$	$0.16 \le T \le 0.864$	$0.864 \le T$
Acceleration (m/s^2)	$0.96 + 9T$	2.40	$2.074/T$

3. Parameter optimization method

The stiffnesses of springs are denoted as K_1, K_2, K_3, K_4, and K_V as shown in Fig 1. Let X_C, X_D, and Y_D denote the X-coordinates of nodes C, D, and the Y-coordinate of node D, respectively. The Z-coordinates of nodes C and D, which have the same value, and the damping coefficient of the vertical damper are denoted by Z_{CD} and C_V, respectively. These ten parameters are chosen as variables to be optimized. Note that the length of the vertical damper is 1 m, and the Y-coordinate of node C is fixed at 0.

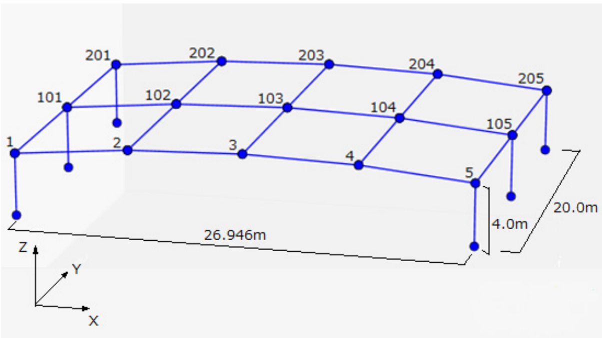

Fig. 2. Latticed shell model; rise = 0.833 m, open angle = 15 deg.

Seismic responses against five sets of seismic motions among 60 sets are evaluated in next section for a latticed shell roof as shown in Fig. 2. Let x_{ji}, y_{ji}, and z_{ji}, denote the X-, Y-, and Z-directional displacements of node j of the roof at the ith step of analysis. The total numbers of analysis steps and nodes are denoted by N_1 and N_2, respectively. The mean value D_{XYZ} of square of the norm of nodal displacements is defined by

$$D_{XYZ} = \frac{1}{N_1 N_2} \sum_{j=1}^{N_2} \sum_{i=1}^{N_1} \{(x_{ji})^2 + (y_{ji})^2 + (z_{ji})^2\} \quad (1)$$

The reduction ratio R_{XYZ} is defined as the ratio of D_{XYZ} with TD-TMD to the value without TMD. Let $\mathbf{D}$ denote the vector consisting of variables. The optimization problem is defined as follows for minimizing the mean value $R_{XYZ}^{\mathrm{mean}}(\mathbf{D})$ of R_{XYZ} among five sets of motions:

Optimization problem of TD-TMD

$$\text{Minimize } R_{XYZ}^{\mathrm{mean}}(\mathbf{D}) \quad (2)$$

subject to bounds for $\mathbf{D}$

4. Optimization result

4.1 Roof model

The TD-TMDs are attached to the latticed roof in Fig. 2. The spans in X- and Y- directions are 26.946 m and 20 m, respectively. The height of column is 4 m, and the roof nodes are located on a circular cylinder with open angle 15 deg. The material is steel, and all beams and columns are connected rigidly at joints. The columns are pin-supported around Y-axis. All of 15 roof nodes have the mass of 500 kg. Although the details of member sections are omitted, the vibration properties of the structure are listed in Table 2.

Table 2. Vibration properties of latticed shell.

Order	Frequency (Hz)	Period (s)	Effective mass ratio (%)		
			X	Y	Z
1	3.34	0.2998	87.68	0	0
2	3.76	0.2661	0	59.19	0
3	4.28	0.2337	0	0	54.92

4.2 Parameter optimization

Parameters of TD-TMD are optimized for the following two cases.

Case 1: A TD-TMD is attached at the center node 103 of the latticed shell. The mass of TD-TMD is 1/20 of the total mass of the roof.

Case 2: Two types of TD-TMDs are attached at nodes 2, 4, 202, 204 and nodes 3, 203, respectively, of the latticed shell. The mass of each TD-TMD is 1/120 of the total mass of the roof.

To prevent numerical difficulty in time-history analysis, the 5% of the total mass of each TD-TMD is placed at nodes B and C; i.e., node D has the 90% of the total mass of TMD.

The number of variables is 10 for Case 1, whereas we have 10 variables for each of two types of TD-TMDs, i.e., 20 variables in total, for Case 2.

The bounds of variables except the damping coefficient are determined by solving an auxiliary optimization problem considering static properties of TD-TMD and the optimal values for SD-TMD. Let $\mathbf{D}^{\mathrm{s}}$ denote a vector consisting of nine variables K_V, K_1, K_2, K_3, K_4, X_C, X_D, Y_D, and Z_{CD}.

The optimal stiffness corresponding to the ith vibration mode $\mathbf{\Phi}_i$ is denoted by K_i^{opt}. The mode $\mathbf{\Phi}_i$ is normalized so that the displacement component at the node of the roof, where the SD-TMD is attached, is equal to 1. Let ω_i, M_i, and m_{TMD} denote the natural circular frequency of the ith node, the equivalent mass corresponding to $\mathbf{\Phi}_i$, and the mass of SD-TMD, respectively. The value of K_i^{opt} is determined as [6]

$$K_i^{\mathbf{opt}} = m_{\mathbf{TMD}} \times \left\{ \omega_i / \left(1 + m_{\mathbf{TMD}} / M_i\right) \right\}^2 \tag{3}$$

Let $\mathbf{u}_i$ denote the vector consisting of the displacements in X-, Y-, and Z-directions of $\mathbf{\Phi}_i$ at the node where the TD-TMD is attached. The static stiffness $K_i(\mathbf{D}^s)$ of the TD-TMD with fixed displacement at node A is evaluated as the norm of force applied at node D in the direction of $\mathbf{u}_i$ divided by the norm of displacement. The nine variables are determined to satisfy the constraint $K_i(\mathbf{D}^\mathbf{S}) = K_i^{\mathbf{opt}}$ $(i = 1,2,3)$.

Furthermore, the damper of the TD-TMD should have enough deformation for any three-directional motion. Therefore, the minimum absolute value $U^{\min}(\mathbf{D}^\mathrm{S})$ of the extensions of the damper against unit static loads at node D in various 13 directions as listed in Table3 and 4 for Cases 1 and 2, respectively. Note that the load numbers 4-13 for Case 1 are the same as those for Case 1.

The auxiliary optimization problem is formulated as

Auxiliary static optimization problem of TD-TMD

Minimize $U^{\min}(\mathbf{D}^\mathrm{S})$ (4)

subject to $K_i(\mathbf{D}^\mathbf{S}) = K_i^{\mathbf{opt}}$, $(i=1,2,3)$

Table 3. Loading direction: Case 1

Load No.	Loading direction
1	(1, 0, 0)
2	(0, 1, 0)
3	(0, 0, 1)
4	(1, 1, 0)
5	(1, -1, 0)
6	(1, 0, 1)
7	(1, 0, -1)
8	(0, 1, 1)
9	(0, 1, -1)
10	(1, 1, 1)
11	(-1, 1, 1)
12	(1, -1, 1)
13	(1, 1, -1)

Table 4. Loading direction: Case 2

Load No.	Loading direction: Type 1 TMDs attached at nodes 2, 4, 202, and 204	Loading direction: Type 2 TMDs attached at nodes 3 and 203
1	(-0.8667, 0, -0.4988)	(-1, 0, 0)
2	(-0.0047, -0.9869, 0.1616)	(0, -0.9823, 0.1874)
3	(0.0238, 0, -0.9997)	(0, 0, -1)

The optimization library SNOPT Ver. 7 [7] is used for solving the auxiliary optimization problem. The optimal values of nine variables for Case 1 are listed in the last column of Table 5. From these values, the lower and upper bounds of the variables for problem (2) are determined as listed in the 2nd and 3rd columns, respectively, in Table 5. The upper and lower bounds of variables for two types of TD-TMDs for Case 2 are listed in Tables 6 and 7, respectively.

Table 5. Ranges of variables and optimal value obtained by solving auxiliary static optimization problem (4): Case 1.

variable	Lower bound	Upper bound	Optimal value of auxiliary static problem (4)
K_v (N/m)	200	1	101.5
K_1 (N/m)	400	200	290.2
K_2 (N/m)	1,000	300	552.5
K_3 (N/m)	2,300	1,300	1,781.2
K_4 (N/m)	150	40	89.9
X_C (m)	1.5	0.8	1.09
X_D (m)	0.7	0.1	0.60
Y_D (m)	0.7	0.1	0.61
Z_CD (m)	-0.2	-0.5	-0.28

Table 6. Ranges of variables and optimal value obtained by solving auxiliary static optimization problem (4): Type 1 TMDs attached at nodes 2, 4, 202, and 204 for Case 2.

Variable	Lower bound	Upper bound	Optimal value of static loading
K_v (N/m)	50	1	2.4
K_1 (N/m)	250	10	147.9
K_2 (N/m)	350	150	266.8
K_3 (N/m)	500	250	385.2
K_4 (N/m)	450	200	335.7
X_C (m)	0.7	0.2	0.51
X_D (m)	0.6	0.2	0.40
Y_D (m)	0.3	0.1	0.14
Z_CD (m)	-0.3	-0.8	-0.58

Table 7. Ranges of variables and optimal value obtained by solving auxiliary static optimization problem (4): Type 2 TMDs attached at nodes 3 and 203 for Case 2.

variable	Lower bound	Upper bound	Optimal value of static loading
K_v (N/m)	50	1	4.6
K_1 (N/m)	250	10	140.6
K_2 (N/m)	450	200	296.5
K_3 (N/m)	600	300	385.2
K_4 (N/m)	450	200	330.3
X_C (m)	0.7	0.3	0.50
X_D (m)	0.5	0.1	0.36
Y_D (m)	0.3	0.1	0.18
Z_CD (m)	-0.6	-0.9	-0.80

The bounds of C_V is determined using the following formula for optimal value of SD-TMD [6]:

$$C_i^{opt} = 2 \times m_{\mathbf{TMD}} \times \omega_i \times \sqrt{\frac{3(m_{\mathbf{TMD}} / M_i)}{8\left(1 + m_{\mathbf{TMD}} / M_i\right)^3}} \text{ , } (i = 1,2,3) \quad (5)$$

To solve problem (2) using heuristic approaches of combinatorial problems, the ten variables are discretized into 21 equally spaced values between their upper and lower bounds.

Since the problem considered here is highly nonlinear, 2000 sets of variables are randomly generated to carry out pure random search (PRS). The eight best objective values obtained by PRS for Cases 1 and 2 are listed in the 2nd and 4th columns, respectively, of Table 8.

The solutions are further improved using the tabu search (TS) [8] which is an extension of local search. The initial solutions are the eight best solutions obtained by PRS, the number of steps is 100, and the number of neighborhood solutions is equal to the number of variables; i.e., 10 for Case 1 and 20 for Case 2. The optimal solutions obtained by PRS followed by TS are listed in Table 9 for Cases 1 and 2.

Table 8. Optimal objective values of eight best solutions obtained by PRS and TS after PRS.

Solution	Case 1		Case 2	
	PRS	TS after PRS	PRS	TS after PRS
1	0.4809	0.4516	0.5065	0.4271
2	0.4855	0.4488	0.5338	0.4302
3	0.4984	0.4493	0.5478	0.4287
4	0.5011	0.4638	0.5525	0.4286
5	0.5034	0.4532	0.5639	0.4248
6	0.5133	0.4558	0.5674	0.5350
7	0.5145	0.4595	0.5706	0.4662
8	0.5153	0.4542	0.5709	0.4992

Table 9. Optimal solutions for Cases 1 and 2.

Variable	Case 1	Case 2	
		Type 1 at nodes 2, 4, 202, 204	Type 2 at nodes 3, 203
K_v (N/m)	76.8	19.7	17.3
K_1 (N/m)	304.8	21.4	55.7
K_2 (N/m)	366.7	197.6	271.4
K_3 (N/m)	1347.6	369.0	485.7
K_4 (N/m)	102.9	307.1	390.5
X_C (m)	1.10	0.39	0.70
X_D (m)	0.19	0.49	0.12
Y_D (m)	0.24	0.26	0.21
Z_{CD} (m)	-0.47	-0.35	-0.80
C_V (Ns/m)	3714	240	200

Following properties are observed for performance of PRS and TS:

- The solutions for Case 1, only 88 solutions among 2000 have the objective value less than 0.6. This means that very limit number of solutions have good performance, and it will be difficult to find a good solution using a local search only.
- The number of steps before obtaining the best solutions of eight trials of TS is between 28 and 98; therefore, better solution may be found if we increase the number of steps.
- The number of neighborhood solutions that is rejected by tabu list is, for example, 1 for the solution 2 of Case 1. Therefore, the neighborhood solutions have not been searched intensively enough.
- Eight trials for each of two cases do not converge to the same solution. The solutions are divided into at least three groups or more on the variable space.
- The objective values are sufficiently reduced by carrying out TS after PRS, which shows the efficiency of the combined approach.
- Some variables have values close to their upper or lower bounds. Therefore, the solution may improve if optimization is carried out again after reassigning the bounds of variables.

4.3 Performances of the optimized TD-TMD

For verification of effectiveness of the proposed TD-TMD, the responses against 60 sets of motions are compared with those of conventional SD-TMD. Note that SD-TMD has three sets of spring, damper, and mass in three directions, respectively, and the mass of each TMD is 1/3 of the total mass of TD-TMD. The SD-TMDs are attached at the same node as TD-TMD; therefore, the total numbers of SD-TMDs are 3 for Case 1, and 18 for Case 2. The theoretical optimal values in Ref. [6] are used for spring stiffness and damping coefficient in each direction assuming that SD-TMDs are installed in the directions of vibration of the node corresponding to dominant modes.

Let R_X, R_Y, and R_Z, denote the squares of the response reduction ratios in X-, Y-, and Z-directions, respectively. The statistical resulds for 60 sets of motions for Cases 1 and 2 are listed in Table 10.

For Case 1, the mean values of R_{XYZ} for TD-TMD and SD-TMD are 0.4856 and 0.4913, respectively. Therefore, TD-TMD has an equivalent performance with SD-TMD, if they are attached at only one node, although the response reductions in Y- and Z-directions storongly depend on the properties of seismic motions. It should be noted here that TD-TMD has only single mass and viscous damper, whereas three SD-TMDs consisting of three masses and dampers should be attached at a node in three directions.

By contrast, Case 2, the mean values of R_{XYZ} for TD-TMD and SD-TMD are 0.4259 and 0.3876, respectively. Therefore, SD-TMD has better performance than TD-TMD.

Table 10. Response reduction ratio for 60 sets of motions.

Case	Model	Ratio	Minimum	Maximum	Mean	Standard deviation
1	TD-TMD	R_{XYZ}	0.3418	0.6543	0.4856	0.0726
		R_X	0.2640	0.5445	0.3846	0.0757
		R_Y	0.3627	1.1046	0.6668	0.1849
		R_Z	0.3558	1.2287	0.7130	0.1609
	SD-TMD	R_{XYZ}	0.3645	0.6240	0.4913	0.0700
		R_X	0.3476	0.6184	0.4827	0.0916
		R_Y	0.4153	0.6767	0.5391	0.1017
		R_Z	0.3711	0.6395	0.4914	0.0658
2	TD-TMD	R_{XYZ}	0.3110	0.5076	0.4259	0.0561
		R_X	0.2530	0.4581	0.3742	0.0655
		R_Y	0.4009	0.6557	0.5200	0.0915
		R_Z	0.4014	0.6849	0.5493	0.0746
	SD-TMD	R_{XYZ}	0.2640	0.5519	0.3876	0.0694
		R_X	0.2740	0.5200	0.3876	0.0825
		R_Y	0.2551	0.6550	0.4164	0.1375
		R_Z	0.2236	0.5624	0.3798	0.0955

Table 11. Response reduction ratio for 60 sets of motion with the level of 1/5 of those used for optimization.

Case	Model	Ratio	Minimum	Maximum	Mean	Standard deviation
1	TD-TMD	R_{XYZ}	0.3396	0.7082	0.4855	0.0820
		R_X	0.2333	0.5588	0.3822	0.0827
		R_Y	0.3442	1.2552	0.6684	0.2293
		R_Z	0.3502	1.2905	0.7307	0.1761
	SD-TMD	R_{XYZ}	0.3645	0.6240	0.4913	0.0700
		R_X	0.3476	0.6184	0.4827	0.0916
		R_Y	0.4153	0.6767	0.5391	0.1017
		R_Z	0.3711	0.6395	0.4914	0.0658
2	TD-TMD	R_{XYZ}	0.3126	0.5208	0.4297	0.0575
		R_X	0.2586	0.4536	0.3762	0.0659
		R_Y	0.4271	0.7084	0.5504	0.0970
		R_Z	0.3703	0.6425	0.5170	0.0691
	SD-TMD	R_{XYZ}	0.2640	0.5519	0.3876	0.0694
		R_X	0.2740	0.5200	0.3876	0.0825
		R_Y	0.2551	0.6550	0.4164	0.1375
		R_Z	0.2236	0.5624	0.3798	0.0955

In order to investigate geometrical nonlinearity of TD-TMD, the response reduction ratios are evaluated for seismic motions with the level of 1/5 of those used for optimization. The statistical results for 60 sets of motions are listed in Table 11. As seen from Tables 10 and 11, the results are almost the same. In this example, the effect of geometrical nonlinearity is negligibly small because the deformation of TD-TMD is small enough such that the relative displacement of mass is about 0.17 m at most.

5. Conclusions

An optimization approach has been proposed for a mass damper called TD-TMD for reduction of seismic responses in three directions using a set of single mass and damper. The objective function is the mean value of response reduction ratio against specified sets of seismic motions. An auxiliary static optimization problem is first solved to determine the appropriate bounds of variables.

It has been demonstrated that the parameters can be effectively optimized using the pure random search followed by the heuristic algorithm called tabu search.

The performance of the proposed TD-TMD has been confirmed in comparison to the three conventional SD-TMDs assigned in each direction. TD-TMD has an equivalent performance with SD-TMDs, if they are attached at a single node. However, the comparison between the TD-TMD and SD-TMD should be discussed considering construction cost and robustness against errors in manufacturing process.

References

[1] T. Igusa and K. Xu, Vibration control using multiple tuned mass dampers, J. Sound Vib., Vol. 175(4), pp. 491-503, 1994.

[2] O. Laven and Y. Daniel, Full resources utilization design of irregular structures using multiple tuned mass dampers, Struct. Multidisc. Optim., Vol. 48, pp. 517-532, 2013.

[3] S. Tsuda and M. Ohsaki, Bi-directional seismic vibration control of spatial structures using passive mass damper consisting of compliant mechanism, Proc. IASS-APCS 2012, Seoul, Paper No. 109, 2012.

[4] M. Ohsaki, S. Tsuda and N. Sugiyama, Parameter optimization of geometrically nonlinear tuned mass damper for multi-directional seismic vibration control, Proc. 13th East Asia-Pacific Conference on Structural Engineering and Construction (EASEC13), Sapporo, Japan, Paper No. A-1-1, 2013.

[5] Open System for Earthquake Engineering Simulation (OpenSees), PEERC, USB, http://opensees.berkeley.edu/.

[6] J. P. D. Hartog, Mechanical Vibrations, Dover Publications, 1985.

[7] P. E. Gill, W. Murray and M. A. Saunders, SNOPT: An SQP algorithm for large-scale constrained optimization, SIAM J. Optim., Vol. 12, pp. 979-1006, 2002.

[8] F. Glover, Tabu search: Part 1, ORSA J. Computing. Vol. 1(3), pp. 190-206, 1989.